Acta Crystallographica Section A
Foundations of Crystallography
ISSN 0108-7673

Received 21 November 2000
Accepted 17 January 2001

Polarization-resolved output analysis of X-ray multiple-wave interaction

Yuri P. Stetsko,[a,d]* Hellmut J. Juretschke,[c] Yi-Shan Huang,[a] Yen-Ru Lee,[a] Tze-Chang Lin[a] and Shih-Lin Chang[a,b]

[a]Department of Physics, National Tsing Hua University, Hsinchu, Taiwan, [b]Synchrotron Radiation Research Center, Hsinchu, Taiwan, [c]Department of Physics, Polytechnic University, Brooklyn, NY 11201, USA, and [d]Chernovtsy State University, Chernovtsy 274012, Ukraine. Correspondence e-mail: stetsko@phys.nthu.edu.tw

The polarization suppression of the interfering components in X-ray multiple-wave interaction is observed for the first time by using a polarization analyzer with an arbitrary inclination of the diffraction plane with respect to that of the investigated crystal. The condition for total suppression of the multiple-wave interaction outside the investigated crystals by a polarization analyzer is derived theoretically from the modified Born approximation. By means of the partial suppression of the strong interfering component, the increase in the visibility of multiple-wave interference is experimentally and theoretically demonstrated. The proposed experimental polarization-resolved technique provides an operational way to enhance the visibility of X-ray multiple-wave interaction outside the investigated crystals for direct phase determination.

1. Introduction

The capability of X-ray multiple-wave diffraction for solving the X-ray phase problem and for the determination of the structure-factor multiplet phases has recently been demonstrated (see the reviews by Chang, 1984, 1987, 1992, 1998; Colella, 1995; Weckert & Hümmer, 1997; and references therein). For a multiple-wave diffraction, the coherent dynamical interaction among the single two-wave reflection and the multiple-wave *Umweg* (detoured) reflection that propagates in the same direction as the two-wave reflection causes a phase dependence of the total diffracted intensity. For a reliable determination of the phases of structure factors, the visibility of X-ray multiple-wave interaction in crystals is of fundamental concern. When the amplitudes of the diffracted waves are not comparable with each other, the visibility of the interference effect is low and the phase determination is unreliable. In other words, the phase-insensitive part of the diffracted intensities plays in this case a dominant role, so that the phase signal is suppressed.

Very recently, Stetsko *et al.* (1999, 2000) have observed the new phenomenon of polarization suppression of strong X-ray *Umweg* multiple waves inside a crystal using a properly chosen wavelength and polarization state of the incident radiation. This phenomenon provides a way of increasing the interference visibility (namely the phase sensitivity) in multiple diffraction by means of partial polarization suppression of the strong *Umweg* interfering component, and thus leads to reliable phase determination. The same enhancement of the interference visibility can also be achieved by partial polarization suppression of the single two-wave reflection when its diffraction strength is comparably stronger than that of the multiple-wave *Umweg* reflection. In the literature, the total polarization suppression of the single two-wave reflection in the case of multiple diffraction has been realised by Kshevetskii *et al.* (1985), where the phenomenon of the indirect excitation (the *Umweg* phenomenon) of the polarization-forbidden reflections was observed (see also Stetsko & Chang, 1997).

The methods of the suppression of X-ray waves inside the investigated crystal have some practical drawbacks. In view of the fact that this kind of suppression can be realised only for certain pre-selected wavelengths, the applicability of the methods is therefore limited by the range of accessible wavelengths of the synchrotron radiation. The necessity of changing the energy of the incident radiation for the investigation in different cases of multiple diffraction is also not practical. Very recently, for reliable phase determination, Juretschke (1998*a*,*b*) proposed consideration of the combinations of the polarization states of the incident and diffracted waves near the three-wave interaction point. In the development of that approach, an operational method of enhancing the interference visibility in multiple diffraction by a partial suppression of the strong wavefield component outside the investigated crystal is proposed in the present paper. The method makes use of a polarization analyzer (with Bragg angle close to 45°) for the diffracted wave with a tunable inclination of its diffraction plane with respect to that of the investigated crystal. This approach, which is widely adopted for the investigation of the polarization aspects of single Bragg

reflection, is employed in the present paper for the first time to investigate X-ray multiple-wave interaction. With the capability of separately suppressing the interfering components in multiple-wave diffraction processes, the proposed method provides an easy way to operate on the visibility of X-ray multiple-wave interaction outside the investigated crystals for direct phase determination. A large number of perfect crystals with appropriate strong reflections can be used as the polarization analyzer. Therefore, in contrast to the method of the suppression of waves inside the crystals, the current method proposed can be practically realised for a wide range of photon energies.

2. Polarization suppression

2.1. Theoretical consideration

Multiple-wave diffraction takes place when several sets of atomic planes simultaneously reflect an incident radiation. In the reciprocal space, this corresponds to the situation when more than two reciprocal-lattice points lie on or close to the surface of the Ewald sphere. In particular, a three-wave (O, G, L) diffraction is conventionally realised by the crystal rotation (the azimuthal ψ scan; see, for example, Renninger, 1937) around the reciprocal-lattice vector $\mathbf{G}$ of the G reflection (the primary reflection) to satisfy Bragg's law also for the additional L reflection (the secondary reflection). In other words, in addition to the reciprocal-lattice points O and G, the azimuthal scan also brings the reciprocal-lattice point L of the secondary reflection onto the surface of the Ewald sphere.

The interaction among the wavefield $\mathbf{D}_{G(2)}$ of the single two-wave primary reflection and the wavefield $\mathbf{D}_{G(um)}$ of the multiple-wave *Umweg* reflection modifies the intensity of the primary reflection. The *Umweg* wave can be considered as the wavefield resulting from a successive scattering from the secondary L through the coupling $G - L$ lattice planes. Within the framework of the second-order Born approximation (see, for example, Stetsko *et al.*, 2000, and references therein), the wavefield $\mathbf{D}_{G(3)}$ of a three-wave (O, G, L) diffraction is given as

$$\begin{aligned}\mathbf{D}_{G(3)} &= \mathbf{D}_{G(2)} + \mathbf{D}_{G(um)} \\ &= A_G \mathbf{s}_G \times \mathbf{s}_G \times [\chi_G \mathbf{D}_O + A_L \chi_{G-L} \chi_L \mathbf{s}_L \times (\mathbf{s}_L \times \mathbf{D}_O)],\end{aligned} \tag{1}$$

where $\mathbf{D}_O$ is the incident wavefield with magnitude D_O, $A_H = K_H^2/[k^2 - K_H^2(1 - \chi_O)]$ (for $H = G, L$) is the resonance term and χ_H (for $H = O, G, L, G - L$) is the Fourier component of the crystal polarizability proportional to the structure factor of the H reflection. Here, $k = 1/\lambda$ and K_H are the magnitudes of the wavevectors in vacuum and inside the crystal, respectively, and $\mathbf{s}_H$ are the unit vectors of the diffracted waves.

For a linearly polarized incident wave $\mathbf{D}_O = D_O \mathbf{p}_O$, the polarization unit vector $\mathbf{p}_O$ with an arbitrary direction is given as

$$\mathbf{p}_O = \alpha \boldsymbol{\sigma} + \beta \boldsymbol{\pi}_O \equiv \cos \omega_O \boldsymbol{\sigma} + \sin \omega_O \boldsymbol{\pi}_O.$$

Here, the polarization unit vectors

$$\boldsymbol{\sigma} \equiv \boldsymbol{\sigma}_O = -[\mathbf{s}_O \times \mathbf{s}_G]/|[\mathbf{s}_O \times \mathbf{s}_G]| \text{ and } \boldsymbol{\pi}_O = [\mathbf{s}_O \times \boldsymbol{\sigma}],$$

where $\mathbf{s}_O$ is the unit vector of the incident wave and ω_O is the angle between $\mathbf{p}_O$ and the $\boldsymbol{\sigma}$ vector (see Fig. 1). The wavefields $\mathbf{D}_{G(2)}$ and $\mathbf{D}_{G(um)}$ are given as

$$\mathbf{D}_{G(2)}(\mathbf{p}_O) = A_G \chi_G \mathbf{p}_{G(2)}(\mathbf{p}_O) D_O, \tag{2a}$$

$$\mathbf{D}_{G(um)}(\mathbf{p}_O) = A_G A_L \chi_{G-L} \chi_L \mathbf{p}_{G(um)}(\mathbf{p}_O) D_O, \tag{2b}$$

where

$$\mathbf{p}_{G(2)}(\mathbf{p}_O) = (\alpha P_G^\sigma \boldsymbol{\sigma} + \beta P_G^\pi \boldsymbol{\pi}_G), \tag{3a}$$

$$\mathbf{p}_{G(um)}(\mathbf{p}_O) = [p_{um}^\sigma(\mathbf{p}_O)\boldsymbol{\sigma} + p_{um}^\pi(\mathbf{p}_O)\boldsymbol{\pi}_G] \tag{3b}$$

are respectively the polarization vectors of the two-wave reflection G and the *Umweg* wave represented in the coordinate system $(\boldsymbol{\sigma}, \boldsymbol{\pi}_G)$, where the polarization unit vector $\boldsymbol{\pi}_G = [\mathbf{s}_G \times \boldsymbol{\sigma}]$. $P_G^\sigma = 1$ and $P_G^\pi = \cos 2\theta_G$ are the polarization factors of the two-wave reflection G, where θ_G is the Bragg angle and

$$p_{um}^\sigma(\mathbf{p}_O) = \alpha p_{um}^\sigma(\boldsymbol{\sigma}) + \beta p_{um}^\sigma(\boldsymbol{\pi}_O), \tag{4a}$$

$$p_{um}^\pi(\mathbf{p}_O) = \alpha p_{um}^\pi(\boldsymbol{\sigma}) + \beta p_{um}^\pi(\boldsymbol{\pi}_O) \tag{4b}$$

are the polarization factors of the *Umweg* wave for the arbitrary polarization vector $\mathbf{p}_O$ of the incident wave. Here,

$$p_{um}^\sigma(\boldsymbol{\sigma}) = P_G^\sigma - (\boldsymbol{\sigma} \cdot \mathbf{s}_L)^2, \tag{5a}$$

$$p_{um}^\pi(\boldsymbol{\sigma}) = -(\boldsymbol{\sigma} \cdot \mathbf{s}_L)(\boldsymbol{\pi}_G \cdot \mathbf{s}_L), \tag{5b}$$

and

$$p_{um}^\sigma(\boldsymbol{\pi}_O) = -(\boldsymbol{\sigma} \cdot \mathbf{s}_L)(\boldsymbol{\pi}_O \cdot \mathbf{s}_L), \tag{6a}$$

$$p_{um}^\pi(\boldsymbol{\pi}_O) = P_G^\pi - (\boldsymbol{\pi}_O \cdot \mathbf{s}_L)(\boldsymbol{\pi}_G \cdot \mathbf{s}_L) \tag{6b}$$

are the polarization factors of the *Umweg* wave for the σ- and π-polarized incident radiation (see also Shen & Finkelstein, 1992; Shen *et al.*, 1995; Stetsko & Chang, 1999), respectively. For simplicity, the argument $\mathbf{p}_O$ of the polarization vectors $\mathbf{p}_{G(2)}(\mathbf{p}_O)$ and $\mathbf{p}_{G(um)}(\mathbf{p}_O)$ is omitted in Fig. 1, where γ is the angle between these vectors.

Consider then the reflection of the diffracted wavefield $\mathbf{D}_{G(3)}$ by a polarization analyzer. The diffracted wave with a unit wavevector $\mathbf{s}_G$ is the incident wave for the analyzer. Let the polarization state of the analyzer be arbitrary with respect to the incident wave, *i.e.* the angle ω_A between the diffraction

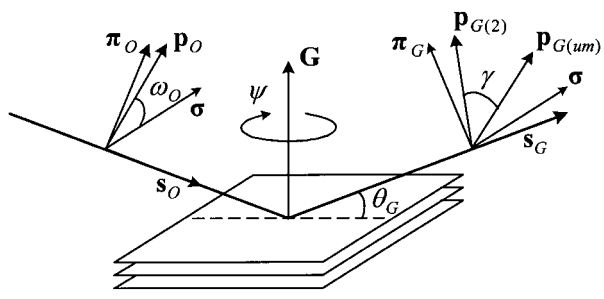

Figure 1
Representation of the polarization vectors for primary G reflection of the three-wave diffraction.

plane of the analyzer and the diffraction plane of the investigated crystal is arbitrary. Fig. 2 shows that the angle ω_A in the coordinate system $(\boldsymbol{\sigma}, \boldsymbol{\pi}_G)$ is the angle between the $\boldsymbol{\sigma}$ vector and the unit polarization vector $\boldsymbol{\sigma}_A$, which is normal to the diffracting plane of the analyzer. The Bragg angle θ_A for the analyzer is close to 45°. Therefore, the π component of the diffracted wave is suppressed (because $\cos 2\theta_A$ is close to zero) and the resulting wavefield $\mathbf{D}^A_{G(3)}$ after the analyzer can be given as

$$\begin{aligned}\mathbf{D}^A_{G(3)} &\equiv \mathbf{D}^A_{G(2)} + \mathbf{D}^A_{G(um)} \\ &= A_A\chi_A[(\mathbf{D}_{G(2)} + \mathbf{D}_{G(um)})\cdot\boldsymbol{\sigma}_A]\boldsymbol{\sigma}_A \\ &= A_A A_G \chi_A(\chi_G \mathbf{p}^{\rm pr}_{G(2)} + A_L\chi_{G-L}\chi_L \mathbf{p}^{\rm pr}_{G(um)})D_O, \quad (7)\end{aligned}$$

where A_A and χ_A are the resonance term and the Fourier component of the crystal polarizability of the reflection used for the analyzer. $\mathbf{p}^{\rm pr}_{G(2)}$ and $\mathbf{p}^{\rm pr}_{G(um)}$, defined as

$$\mathbf{p}^{\rm pr}_{G(2)} = [\mathbf{p}_{G(2)}(\mathbf{p}_O)\cdot\boldsymbol{\sigma}_A]\boldsymbol{\sigma}_A, \quad (8a)$$

$$\mathbf{p}^{\rm pr}_{G(um)} = [\mathbf{p}_{G(um)}(\mathbf{p}_O)\cdot\boldsymbol{\sigma}_A]\boldsymbol{\sigma}_A, \quad (8b)$$

are the projections of the polarization vectors $\mathbf{p}_{G(2)}(\mathbf{p}_O)$ and $\mathbf{p}_{G(um)}(\mathbf{p}_O)$ on the $\boldsymbol{\sigma}_A$ vector. Fig. 2 shows these projections for two qualitatively different cases, (I) and (II), for the $\boldsymbol{\sigma}_A$ vector, considered in detail in §3.3. These two cases are shown in Fig. 2 with appropriate superscripts for the $\boldsymbol{\sigma}_A$ vector.

By the proper choice of the polarization state, *i.e.* the polarization angle ω_A of the analyzer, the directly excited $\mathbf{D}_{G(2)}$ or the *Umweg*-exited $\mathbf{D}_{G(um)}$ wavefields can be suppressed when the length of the projections $\mathbf{p}^{\rm pr}_{G(2)}$ or $\mathbf{p}^{\rm pr}_{G(um)}$ is close or equal to zero. Thus, the total (exact) suppression of the primary or the *Umweg* waves can be realised when the $\boldsymbol{\sigma}_A$ vector of the analyzer is normal to the vectors $\mathbf{p}_{G(2)}(\mathbf{p}_O)$ or $\mathbf{p}_{G(um)}(\mathbf{p}_O)$, respectively.

In general, the angle γ between the vectors $\mathbf{p}_{G(2)}(\mathbf{p}_O)$ and $\mathbf{p}_{G(um)}(\mathbf{p}_O)$ (see Fig. 1), which depends on the wavelength and the polarization state ω_O of the incident wave, can be arbitrary. So the vectors $\mathbf{p}_{G(2)}(\mathbf{p}_O)$ and $\mathbf{p}_{G(um)}(\mathbf{p}_O)$ are generally not collinear. Therefore, by the proper choice of the polarization state ω_A of the analyzer, the primary and the *Umweg* waves after the investigated crystal can be suppressed separately.

2.2. Experimental

The experiments using a polarization analyzer for suppression of a strong primary or an *Umweg* wave in multiple-wave conditions were carried out at the wiggler beamline BL-17B of the Synchrotron Radiation Research Center (see, for example, Chang *et al.*, 1998). The synchrotron storage ring was operating at 1.5 GeV and 200 mA. The vertical and horizontal angular divergences of the beam after the double-crystal Si(111) monochromator and the focusing and collimation systems were 0.010 and 0.025°, respectively. The crystal was aligned on an eight-circle Huber diffractometer. Fig. 3 shows the experimental diffraction geometry that provided a variable polarization state ω_O of the incident radiation (along the x axis) by changing the orientation of the investigated crystal relative to the incident polarized electric field (along the y axis). The standard supporting system of the diffractometer was modified in such a way to provide the joint rotation ω_A of the analyzer and the detector around the direction of propagation (along the $\mathbf{s}_G$ vector) of the diffracted wave G. This rotation could be carried out without introducing changes to the angle of incidence for the diffracting planes of the analyzer. The wavelength 1.5399 Å of the incident radiation was selected so that the Bragg angle $\theta_A = 45.001°$ of the Ge(333) reflection of the analyzer was close to 45°. Multiple-wave diffractions were then performed by rotating the investigated crystal around the $\mathbf{G}$ vector *via* the ψ scan for different polarization states ω_A of the analyzer.

The most interesting cases of suppression involve a weak primary and a strong *Umweg* reflection and *vice versa*. For a weak primary and a strong *Umweg* reflection (the first case), the $|\chi_{G-L}|$ of the coupling and $|\chi_L|$ of the secondary reflections in $\mathbf{D}_{G(um)}$ are much greater than the $|\chi_G|$ of the primary reflection in $\mathbf{D}_{G(2)}$. For the opposite situation (the second case), *i.e.* a strong primary and a weak *Umweg* reflection, the $|\chi_G|$ in $\mathbf{D}_{G(2)}$ is much greater than either of the $|\chi_{G-L}|$ and $|\chi_L|$ in $\mathbf{D}_{G(um)}$. In both cases, the strong component can be weakened by properly choosing the polarization state ω_A of the analyzer so that its amplitude would be totally suppressed or comparable with that of the weaker component.

2.2.1. Weak primary and strong *Umweg* reflections. Consider the first case, the three-wave diffraction GaAs (000, $\bar{2}\bar{2}\bar{2}$, $\bar{3}\bar{1}3$), with a weak primary reflection ($\bar{2}\bar{2}\bar{2}$) and strong

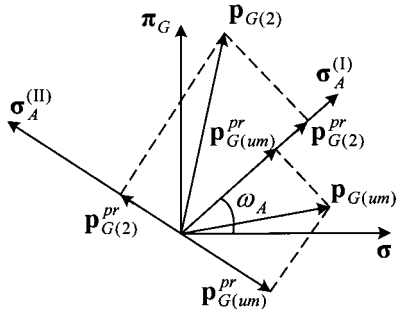

Figure 2
Representation of the polarization vectors in the coordinate system $(\boldsymbol{\sigma}, \boldsymbol{\pi}_G)$ in the scheme with polarization analyzer.

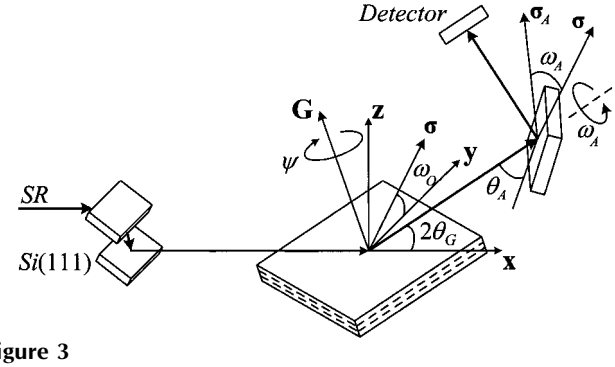

Figure 3
The diffraction geometry of the experiment.

secondary ($\bar{3}\bar{1}3$) and coupling ($1\bar{1}\bar{5}$) reflections. Fig. 4 shows the experimental intensity profiles for the π-polarized ($\omega_O = 90^\circ$) incident radiation and different values of the polarization state ω_A of the analyzer. The positive direction of the azimuthal rotation $\Delta\psi$ in Fig. 4, the same as in Figs. 5–9, corresponds to the movement of the reciprocal-lattice point of the secondary reflection L towards the interior of the Ewald sphere (see, for example, Stetsko & Chang, 1999). For the regions $-90 \le \omega_A < -60^\circ$ and $20 < \omega_A \le 90^\circ$, the intensity profiles (not shown) are qualitatively the same as those in Figs. 4(*a*) and 4(*c*). Under the experimental conditions, the wavelength and polarization state of the incident radiation, the angles γ, $\omega_{G(2)}$ and $\omega_{G(um)}$ are 21, 90 and 69°, respectively, where $\omega_{G(2)}$ and $\omega_{G(um)}$ are the angles between the $\boldsymbol{\sigma}$ vector and the $\mathbf{p}_{G(2)}$ and $\mathbf{p}_{G(um)}$ vectors.

For the polarization states of the analyzer, $\omega_A = \pm 90^\circ$, the $\boldsymbol{\sigma}_A$ vector is collinear with the $\mathbf{p}^{\rm pr}_{G(2)}$ vector. Therefore, in these cases, the weak primary diffracted wave is not suppressed by the analyzer ($c_{G(2)} \equiv |\mathbf{p}^{\rm pr}_{G(2)}|/|\mathbf{p}_{G(2)}| = 1$) while the strong *Umweg* diffracted wave is slightly suppressed ($c_{G(um)} \equiv |\mathbf{p}^{\rm pr}_{G(um)}|/|\mathbf{p}_{G(um)}| = 0.93$). The increasing of the ω_A angle from -90 to -21° is accompanied by the gradual

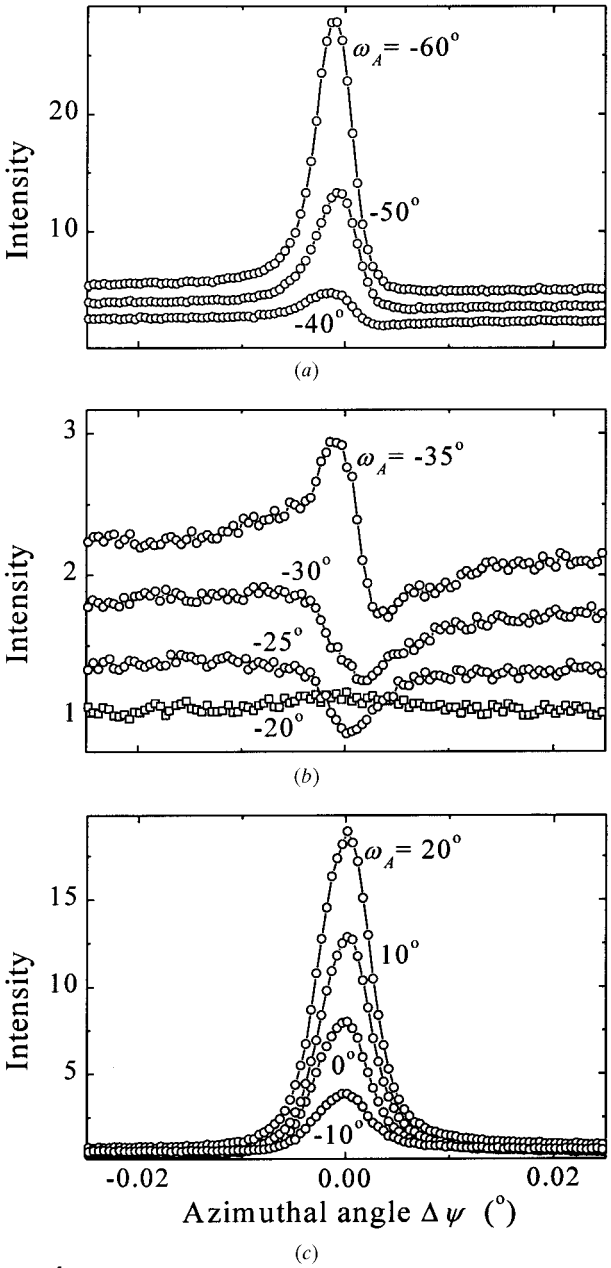

Figure 4
Intensity profiles of GaAs(000, $\bar{2}\bar{2}\bar{2}$, $\bar{3}\bar{1}3$) three-wave diffraction for the π-polarized incident radiation and for different values of the polarization state ω_A of the analyzer. Intensities are normalized with the two-wave intensity at $\omega_A = -20^\circ$.

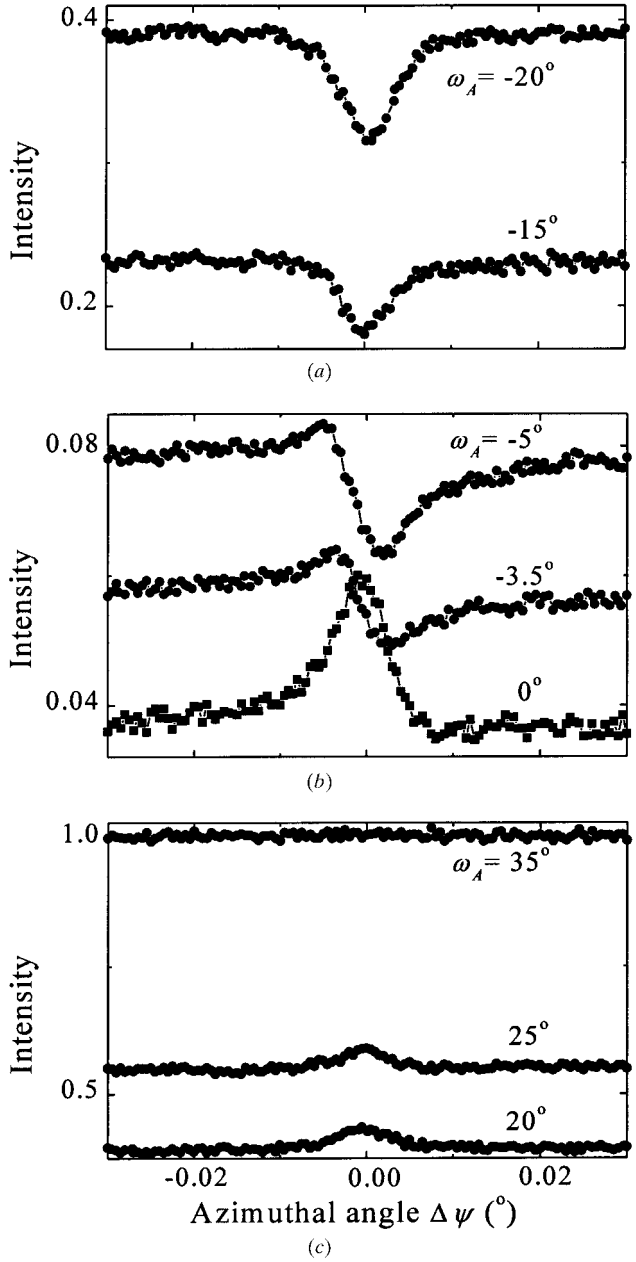

Figure 5
Intensity profiles of GaAs(000, 111, $33\bar{1}$) three-wave diffraction for the π-polarized incident radiation and for different values of the polarization state ω_A of the analyzer. Intensities are normalized with the two-wave intensity at $\omega_A = 35^\circ$.

suppression (see Figs. 4*a* and 4*b*) of the *Umweg* wave, *i.e.* the decreasing of the intensity of the *Umweg* peak. The total suppression ($c_{G(um)} = 0$) occurs around $\omega_A = -21^\circ$, which is characterized by the practical absence of the deviation of the three-wave intensity from the two-wave intensity. The further increasing of ω_A (see Fig. 4*c*) tends to increase the intensity of the *Umweg* peak. Correspondingly, the primary diffracted wave is totally suppressed ($c_{G(2)} = 0$) around $\omega_A = 0^\circ$, while it is less suppressed ($c_{G(2)} = 0.36$) for $\omega_A = -21^\circ$. Thus, the primary and the *Umweg* waves are totally suppressed at different polarization states ω_A of the analyzer.

2.2.2. Strong primary and weak *Umweg* reflections. Consider the second case, the three-wave diffraction GaAs(000, 111, $33\bar{1}$), with a strong primary (111) reflection, a strong secondary ($33\bar{1}$) and a weak coupling ($\bar{2}\bar{2}2$) reflection, *i.e.* the *Umweg* reflection is weak. Fig. 5 shows the experimental intensity profiles for the π-polarized incident radiation and different values of the polarization state ω_A of the analyzer. The angles are $\gamma = 36.5^\circ$, $\omega_{G(2)} = 90^\circ$ and $\omega_{G(um)} = 126.5^\circ$. For the regions $-90 \leq \omega_A < -20^\circ$ and $35 < \omega_A \leq 90^\circ$, the intensity profiles (not shown) are qualitatively the same as that in Fig. 5(*a*), where the intensity profiles are of the *Aufhellung* type (Wagner, 1923), *i.e.* three-wave intensity is lower than the two-wave intensity. For the polarization states of the analyzer, $\omega_A = \pm 90^\circ$, the strong primary diffracted wave is not suppressed, while the weak *Umweg* diffracted wave is slightly suppressed ($c_{G(um)} = 0.8$). The increase of ω_A angle from -90 to 0° is accompanied by the suppression of the primary wave (see Figs. 5*a–c*) together with a change from the *Aufhellung* type (dip) to the *Umweg* type (peak) intensity profile. The total suppression of the primary wave ($c_{G(2)} = 0$) occurs around $\omega_A = 0^\circ$ while for the *Umweg* wave ($c_{G(um)} = 0$) it is observed around $\omega_A = 36.5^\circ$. Again, the total suppression of the *Umweg* wave is characterized by the practical absence of the deviation of the three-wave intensity from two-wave intensity.

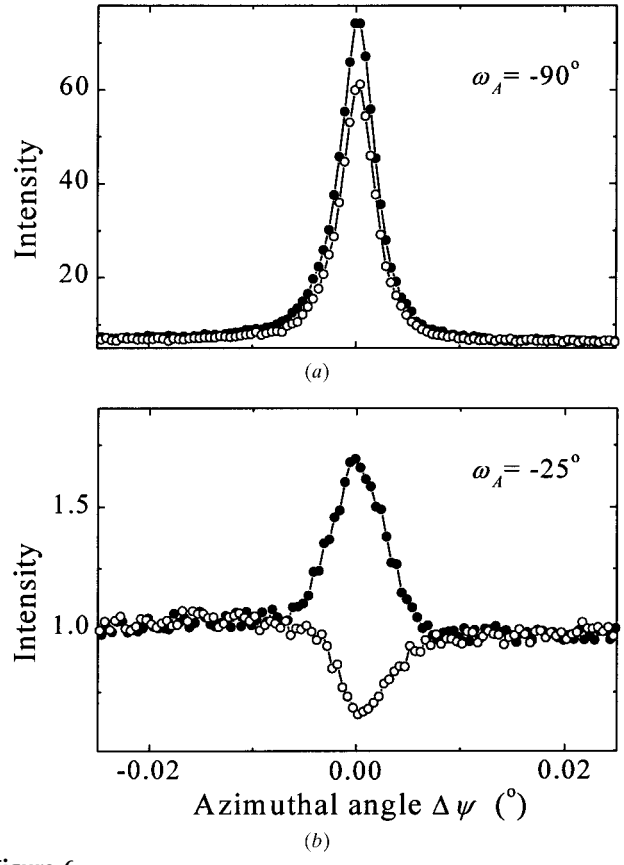

Figure 6
Intensity profiles of GaAs(000, 222, $31\bar{3}$) (solid circles) and GaAs(000, $\bar{2}\bar{2}\bar{2}$, $\bar{3}1\bar{3}$) (open circles) three-wave diffractions for the π-polarized incident radiation and the polarization states (*a*) $\omega_A = -90^\circ$ and (*b*) $\omega_A = -25^\circ$ of the analyzer. Intensities are normalized with the two-wave intensity at $\omega_A = -25^\circ$.

3. Phase sensitivity

3.1. Qualitative increase of phase sensitivity with suppression

3.1.1. Theoretical consideration. The total suppression of either of the two interfering components is accompanied by the complete reduction of the phase sensitivity of multiple-wave interaction (see also Stetsko *et al.*, 2000). However, in cases when one of the components is much stronger than the other, *i.e.* the phase sensitivity is low, the partial suppression of the strong component by the analyzer can provide comparable amplitudes for interference, thus the phase sensitivity of the multiple-wave interaction increases qualitatively.

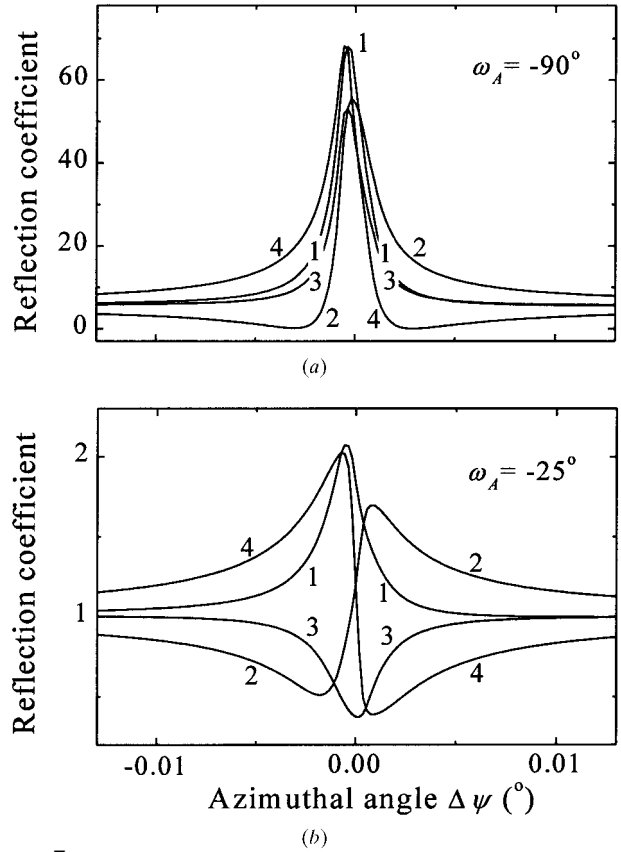

Figure 7
Calculated profiles of Fig. 5. Curves 1, 2, 3 and 4 correspond to $\delta_3 = -90$, 0, 90 and 180°, respectively.

According to the second-order Born approximation given in Chang & Tang (1988), Chang *et al.* (1989) and Stetsko *et al.* (2000), the relative intensity $I^A_{G(3)}/I^A_{G(2)} = |\mathbf{D}^A_{G(3)}|^2/|\mathbf{D}^A_{G(2)}|^2$ after the analyzer *versus* the reduced azimuthal angle parameter $\varphi = 2\Delta\psi/\eta$ can be expressed as

$$I^A_{G(3)}/I^A_{G(2)} = 1 + A^{-1}F[B(\varphi\cos\delta_3 - \sin\delta_3) + FC]/(\varphi^2 + 1), \tag{9}$$

where $\eta = |\chi_O|/(\boldsymbol{\sigma}\cdot\mathbf{s}_L)\cos\theta_G$ is the fundamental width (see Chang *et al.*, 1989) of the three-wave diffraction, $\delta_3 = \delta_L + \delta_{G-L} - \delta_G$ is the triplet phase of the structure-factor triplet F_LF_{G-L}/F_G and $F = |F_{G-L}||F_L|/(|F_O||F_G|)$, $A = |\mathbf{p}^{\rm pr}_{G(2)}|^2$, $B = (\mathbf{p}^{\rm pr}_{G(2)}\cdot\mathbf{p}^{\rm pr}_{G(um)})$, $C = |\mathbf{p}^{\rm pr}_{G(um)}|^2$.

Similar to the paper by Stetsko *et al.* (2000), for high phase sensitivity (see also Weckert *et al.*, 1993; Weckert & Hümmer, 1997), the value $|B|$ of (9) has to be comparable with FC and more than FC, *i.e.* the parameter

$$S \equiv FC/|B| \leq 1. \tag{10}$$

For the case involving a weak primary and a strong *Umweg* reflection, the value of FC is much larger than $|B|$ ($S \gg 1$) when the polarization state ω_A of the analyzer is far from the suppression condition for the *Umweg* wave. According to Chang & Tang (1988) and Chang *et al.* (1989), this case is of low phase sensitivity owing to the large value of the phase-independent component. On the other hand, for the polarization states ω_A close to the condition of the total suppression of the *Umweg* wave, the values S, FC and B are close to zero. These cases are also of low phase sensitivity owing to the low visibility of the three-wave intensity profiles on the background of the two-wave intensity. The intermediate situation ($S \leq 1$) is realised when the *Umweg* wave is partially suppressed by the analyzer. Under this condition, the $|\mathbf{p}^{\rm pr}_{G(2)}|$ of (7) is comparable with $F|\mathbf{p}^{\rm pr}_{G(um)}|$. Thus, in comparison with the cases $S \gg 1$ and $S = 0$, a qualitative increase in phase sensitivity for the three-wave intensity profiles is achieved.

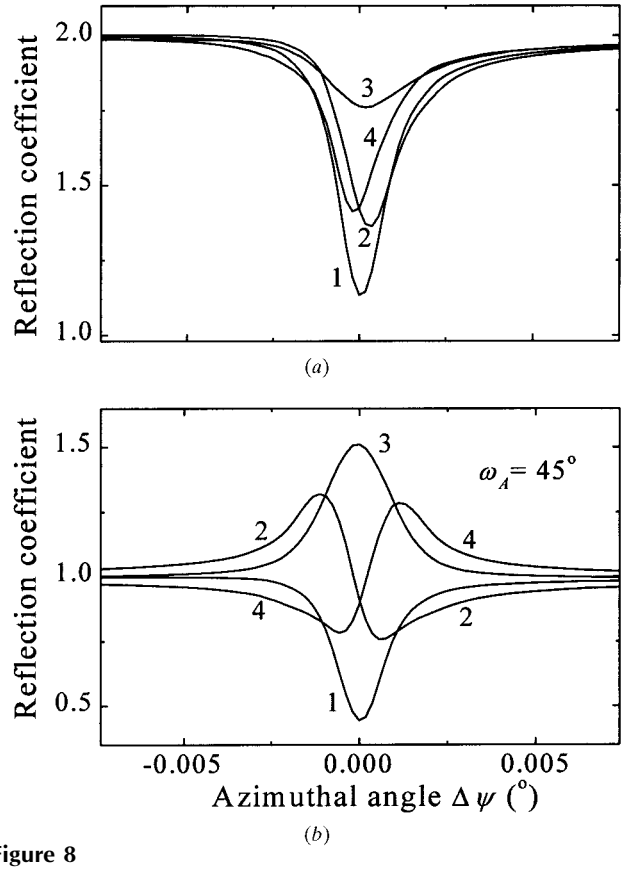

Figure 8
Calculated profiles for Si(000, 311, 404) three-wave diffraction for the π-polarized incident radiation (*a*) without analyzer and (*b*) at the polarization state ω_A = 45° of the analyzer. Curves 1, 2, 3 and 4 correspond to δ_3 = −90, 0, 90 and 180°, respectively. Intensities are normalized with the two-wave intensity of case (*a*).

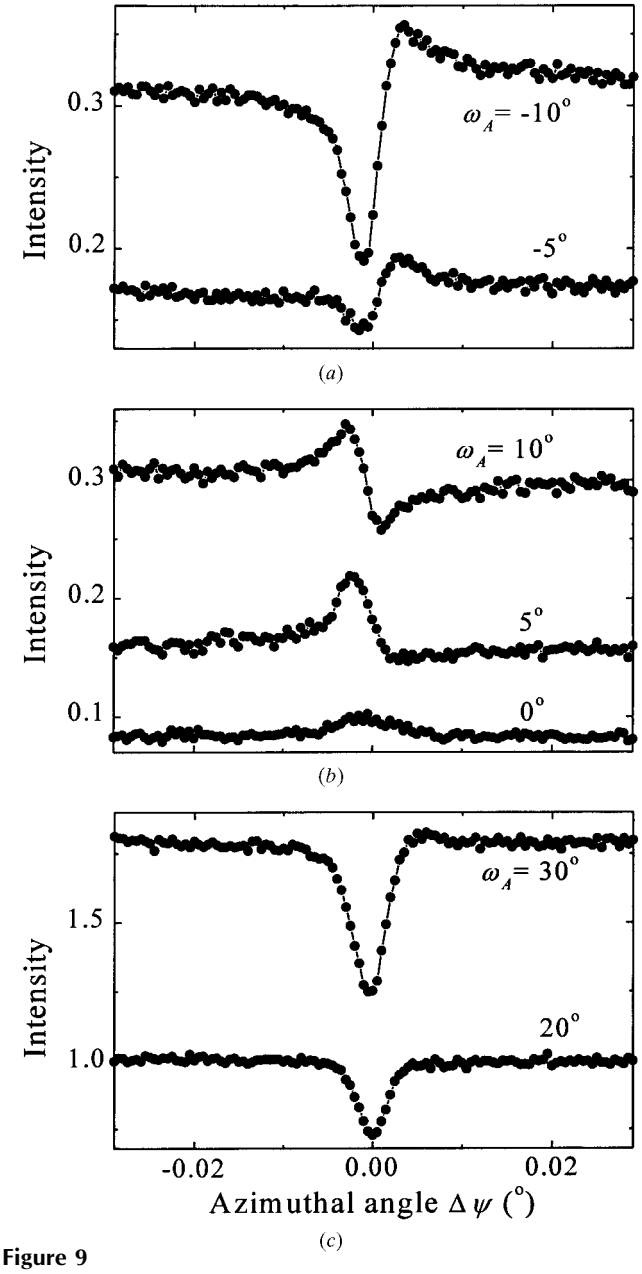

Figure 9
Intensity profiles of GaAs(000, 111, 220) three-wave diffraction for the π-polarized incident radiation and for different values of the polarization state ω_A of the analyzer. Intensities are normalized with the two-wave intensity at ω_A = 20°.

It should be noted that the second-order Born approximation and the condition (10) for quantitative estimation of the phase sensitivity of three-wave diffraction are valid for the cases with comparably weak primary reflections. According to Chang & Tang (1988), for multiple-wave diffraction with a strong primary reflection it is necessary to use a higher-order approximation [see also the second-order perturbation solution to the Takagi–Taupin equations by Thorkildsen (1987); and in a simplified version by Mathiesen *et al.* (1998)]. This point is not considered in the present paper. However, from the common point of view, high phase sensitivity is also expected when $|\mathbf{p}^{\rm pr}_{G(2)}|$ is comparable with $F|\mathbf{p}^{\rm pr}_{G(um)}|$.

3.1.2. Experimental and dynamical calculations. The qualitative increase in phase sensitivity is verified experimentally for two three-wave diffraction cases: (+) GaAs[$O(000)$, $G(222)$, $L(31\bar{3})$] and (−) GaAs[$O(000)$, $-G(\bar{2}\bar{2}\bar{2})$, $-L(\bar{3}\bar{1}3)$] (for the latter, see §2.2.1) with weak primary and strong *Umweg* reflections. These cases are related by the symmetry of inversion (see, for example, Hümmer *et al.*, 1989, 1990; Chang *et al.*, 1999), *i.e.* the triplet phases $\delta_3^{(-)} = -\delta_3^{(+)}$ for negligibly small anomalous dispersion. Fig. 6 shows the experimental intensity profiles [case (+) solid circles; case (−) open circles] for π-polarized incident radiation and for the polarization states $\omega_A = -90$ and -25° of the analyzer. The polarization state $\omega_A = -25^\circ$ is chosen to satisfy the condition for high phase sensitivity, $S = 0.79$. Accordingly, $S = 4.4$ for the polarization state $\omega_A = -90^\circ$. For comparison, Fig. 7 shows the intensity profiles calculated for artificially assigned δ_3 values (Weckert & Hümmer, 1997; Stetsko & Chang, 1999) using the dynamical theory without approximation (Stetsko & Chang, 1997). For the polarization state $\omega_A = -90^\circ$, rather low phase sensitivity is observed in Figs. 6(*a*) and 7(*a*), where the *Umweg* phenomenon dominates. The curves calculated for $\delta_3 = -90$ and 90° (see Fig. 7*a*) are symmetrical and very similar (*Umweg* type), while those for $\delta_3 = 0$ and 180° are slightly asymmetrical. Similarly, low phase sensitivity of intensity profiles is observed (not shown in the figures) for cases without analyzer, where parameter $S = 5.1$ (see Stetsko *et al.*, 2000). Figs. 6(*b*) and 7(*b*) show the well known shapes of the intensity profiles for the high phase-sensitive case (see, for example, Weckert & Hümmer, 1997; Chang, 1998), where the partial suppression of the strong *Umweg* component is realised for $\omega_A = -25^\circ$. The intensity profiles calculated for $\delta_3 = 0$ and 180° (curves 2 and 4 in Fig. 7*b*, respectively) are asymmetric with comparably large maximum and minimum intensity deviations from the intensity of the two-wave case. The intensity profiles calculated for $\delta_3 = -90$ and 90° are practically symmetric with different extremum intensity deviations (maximum for curve 1 and minimum for curve 3 in Fig. 7*b*, respectively) from the intensity of the two-wave case. The further total suppression of the *Umweg* component, when $S = 0$, leads again to low phase sensitivity [see the curve for $\omega_A = -20^\circ$ in Fig. 4(*b*)].

The region, $-35 \le \omega_A \le -25^\circ$ (see Fig. 4*b*), of high phase sensitivity is rather narrow and close to the polarization state $\omega_A = -21^\circ$ of the total suppression of the *Umweg* wave. As follows from (10), the angular range of this region and the difference from the ω_A value for total suppression depend on the relationship between the structure factors and the polarization factors of the primary and the *Umweg* waves. If the structure factors of the waves are very different from one another (much more different than in the cases considered here), so that at least one of the reflections is very weak or forbidden, the range and the difference in ω_A from the state of total suppression are negligibly small. In these extreme cases, the proposed method cannot be used practically. For the case involving a strong primary and a weak *Umweg* reflection (see §2.2.2), which is not considered in detail here, the angular region $-7 \le \omega_A \le -3^\circ$ (see Fig. 5*b*) of high phase sensitivity is also rather narrow and close to the polarization state $\omega_A = 0^\circ$ of the total suppression of the primary wave.

3.2. Qualitative increase of phase sensitivity without suppression

The additional opportunity of the proposed method to increase the phase sensitivity is theoretically considered in this section. In the case involving all comparably strong reflections, the three-wave diffraction is conventionally considered as a phase-sensitive diffraction. However, for some wavelengths and polarization states ω_O of the incident radiation, the situation with the angle γ between the polarization vectors $\mathbf{p}_{G(2)}$ and $\mathbf{p}_{G(um)}$ close to 90° can be realised. In this case, the amplitude of the phase-sensitive part of the intensity, proportional to the scalar product of these vectors (see, for example, Stetsko *et al.*, 2000) is close to zero and the phase sensitivity of the three-wave diffraction is low. For example, for the Si(000, 311, 404) three-wave diffraction and the π-polarized ($\omega_O = 90^\circ$) incident Cu $K\alpha_1$ radiation, the angle $\gamma = 100.3^\circ$ is rather close to 90°. The corresponding angles are $\omega_{G(2)} = 90^\circ$ and $\omega_{G(um)} = 190.3^\circ$. Fig. 8(*a*) shows the calculated intensity profiles for this case. Rather low phase sensitivity is observed, where the *Aufhellung* component dominates in the intensity.

In contrast to the present case where the length of the projection of the polarization vector $\mathbf{p}_{G(2)}$ on $\mathbf{p}_{G(um)}$ or *vice versa* is close to zero, the polarization state ω_A in the experimental scheme with an analyzer can be chosen so that the lengths of the projections $\mathbf{p}^{\rm pr}_{G(2)}$ and $\mathbf{p}^{\rm pr}_{G(um)}$ [of the vectors $\mathbf{p}_{G(2)}$ and $\mathbf{p}_{G(um)}$ on $\boldsymbol{\sigma}_A$, respectively, see Fig. 2] are comparably large. Fig. 8(*b*) shows the intensity profiles calculated for the polarization state $\omega_A = 45^\circ$. The high phase sensitivity of the profiles is observed. For the considered case with all comparably strong reflections, the angular width of the region, $20 \le \omega_A \le 60^\circ$, of high phase sensitivity is more than that of the previous cases and farther from the polarization states $\omega_A = 0$ and $\omega_A = 100.3^\circ$, respectively, of the total suppression of the primary and of the *Umweg* waves.

Certainly, there is no practical necessity to use an analyzer for obtaining the high phase-sensitive conditions for such a type of three-wave diffraction. In fact, it is easier to change the energy or the polarization state ω_O of the incident radiation to make the angle γ rather different from 90°. However, the above-mentioned possibility of low phase sensitivity has to be

taken into account, especially when a large number of multiple diffraction situations are investigated using a fixed common photon energy and polarization state of the incident radiation. For example, in a conventional X-ray laboratory, only some specific energies, in particular Cu $K\alpha$, can be used. As to the polarization state of the incident radiation of the synchrotron and the laboratory source, the π-polarized radiation after the monochromator is usually preferable to the σ-polarized radiation owing to better beam resolution in the azimuthal direction of the crystal rotation during the generation of multiple-wave diffraction.

3.3. Inversion of intensity profile asymmetry

The inversed asymmetry, the so-called anomalous asymmetry, of three-wave intensity profiles for π-polarized incident radiation compared with that for σ-polarized radiation was detected by Juretschke (1986) (see also Weckert & Hümmer, 1997; Larsen & Thorkildsen, 1998; Stetsko & Chang, 1999). When the signs of the polarization factors P_G^{π} and p_{um}^{π} ($\boldsymbol{\pi}_O$) of the primary and *Umweg* reflections for π-polarized incident radiation are different, an additional 180° phase shift is introduced in the diffraction process and the inversion of the profile asymmetry occurs. In particular, this phase shift is observed for the low sensitive case shown in Fig. 8(a), where the angle γ is more than 90°.

The inversion of the profile asymmetry also takes place in the experimental scheme with analyzer but the geometry situation is different from the cases already reported in the literature. Fig. 2 shows two qualitatively different polarization states ω_A of the analyzer with two positions $\sigma_A^{(\mathrm{I})}$ and $\sigma_A^{(\mathrm{II})}$ of the polarization vector for the respective cases: (I) when the direction of the projection of the $\mathbf{p}_{G(2)}$ vector on the $\sigma_A^{(\mathrm{I})}$ vector coincides with that of the $\mathbf{p}_{G(um)}$ vector, *i.e.* $(\mathbf{p}_{G(2)}^{\mathrm{pr}} \cdot \mathbf{p}_{G(um)}^{\mathrm{pr}}) > 0$, and (II) when the direction of the projection of the $\mathbf{p}_{G(2)}$ vector on the $\sigma_A^{(\mathrm{II})}$ vector is opposite to that of the $\mathbf{p}_{G(um)}$ vector, *i.e.* $(\mathbf{p}_{G(2)}^{\mathrm{pr}} \cdot \mathbf{p}_{G(um)}^{\mathrm{pr}}) < 0$. In case (I), owing to the positive value of B in (9), the asymmetry of intensity profiles is the same as that conventionally obtained for σ-polarized incident radiation in the experimental scheme without analyzer. In case (II), owing to the negative value of B, an inversion of the peak profile asymmetry takes place in comparison with case (I). This inversion happens every time when the polarization state ω_A of the analyzer crosses the polarization states of the total suppression of the primary or the *Umweg* waves.

The inversion of profile asymmetry is experimentally verified for GaAs(000, 111, 220) three-wave diffraction with all strong reflections involved. Fig. 9 shows the experimental intensity profiles for the π-polarized incident radiation and for different values of the polarization state ω_A of the analyzer. For the angular regions $-90 \leq \omega_A < -10°$ and $30 < \omega_A \leq 90°$, the intensity profiles (not shown) are qualitatively the same as that in Fig. 9(a). The corresponding angles are $\gamma = 17.1°$, $\omega_{G(2)} = 90°$ and $\omega_{G(um)} = 107.1°$. In case (II) when $0 \leq \omega_A < 17.1°$, the inversed asymmetry (see Fig. 9b) compared with that (see Figs. 9a and 9c) outside this angular region is observed. The same inversed asymmetry of intensity profiles is also shown in Fig. 8(b), where the situation corresponding to case (II) for the polarization state $\omega_A = 45°$ of the analyzer is realised.

For the considered three-wave diffraction with all strong reflections involved, the *Aufhellung* phenomenon is observed [see the curve for $\omega_A = 20°$ in Fig. 9(c)] under the total suppression of the *Umweg* wave. This differs from the experimental results presented in §§2.2.1 and 2.2.2 of the paper, where the *Aufhellung* phenomenon is practically reduced [see the curve for $\omega_A = -20°$ in Fig. 4(b) and the curve for $\omega_A = 35°$ in Fig. 5(c)]. Probably the latter can be explained by the presence of one of the weak reflections in the three-wave diffraction as well as the geometry (polarization factors) of this diffraction. It can be more correctly described within the framework of the third-order Born approximation or the second-order perturbation solution to the Takagi–Taupin equations.

It should be noted that the considered conditions of the suppression of waves in the multiple-wave interaction are obtained using only geometrical factors within the framework of the Born approximation. Therefore, the angular positions ω_A of the suppression obtained according to these conditions can differ in several arc degrees from that observed experimentally or from the values calculated using the dynamical theory.

In conclusion, a polarization analyzer with an arbitrary polarization state with respect to the diffraction plane of the crystal is used for the first time to investigate X-ray multiple-wave interaction. By choosing an appropriate polarization state of the analyzer, the suppression of each of the interfering components outside the investigated crystals is observed. A method for qualitative enhancement of phase sensitivity in multiple-wave interaction using partial suppression of a stronger interfering component is proposed. This polarization-resolved method may provide an operational way to increase the visibility of X-ray multiple-wave interaction outside the investigated crystals for effective determination of X-ray reflection phases.

The authors are indebted to the Ministry of Education and the National Science Council for financial support under contract no. 90-FA04-AA. YPS, YSH and YRL are very grateful to the same organizations for providing a visiting scholarship and graduate fellowships during the course of this study.

References

Chang, S. L. (1984). *Multiple Diffraction of X-rays in Crystals.* Heidelberg: Springer-Verlag.
Chang, S. L. (1987). *Crystallogr. Rev.* **1**, 87–189.
Chang, S. L. (1992). *Int. J. Mod. Phys.* B**6**, 2987–3020.
Chang, S. L. (1998). *Acta Cryst.* A**54**, 886–894.
Chang, S. L., Huang, Y. S., Chao, C. H., Tang, M. T. & Stetsko, Yu. P. (1998). *Phys. Rev. Lett.* **80**, 301–304.
Chang, S. L., Huang, M. T., Tang, M. T. & Lee, C. H. (1989). *Acta Cryst.* A**45**, 870–878.
Chang, S. L., Stetsko, Yu. P., Huang, Y. S., Chao, C. H., Liang, F. J. & Chen, C. K. (1999). *Phys. Lett. A*, **264**, 328–333.

Chang, S. L. & Tang, M. T. (1988). *Acta Cryst.* A**44**, 1065–1072.
Colella, R. (1995). *Comm. Condens. Matter Phys.* **17**, 175–215.
Hümmer, K., Weckert, E. & Bondza, H. (1989). *Acta Cryst.* A**45**, 182–187.
Hümmer, K., Weckert, E. & Bondza, H. (1990). *Acta Cryst.* A**46**, 393–402.
Juretschke, H. J. (1986). *Phys. Status Solidi B*, **135**, 455–466.
Juretschke, H. J. (1998*a*). *Cryst. Res. Technol.* **33**, 569–581.
Juretschke, H. J. (1998*b*). Private communication.
Kshevetskii, S. A., Stetsko, Yu. P. & Shelud'ko, S. A. (1985). *Sov. Phys. Crystallogr.* **30**, 270–272.
Larsen, H. B. & Thorkildsen, G. (1998). *Acta Cryst.* A**54**, 129–136.
Mathiesen, R. H., Mo, F., Eikenes, A., Nyborg, T. & Larsen, H. B. (1998). *Acta Cryst.* A**54**, 338–347.
Renninger, M. (1937). *Z. Kristallogr.* **97**, 107–121.
Shen, Q. & Finkelstein, K. D. (1992). *Phys. Rev. B*, **45**, 5075–5078.
Shen, Q., Shastri, S. & Finkelstein, K. D. (1995). *Rev. Sci. Instrum.* **66**, 1610–1613.
Stetsko, Yu. P. & Chang, S. L. (1997). *Acta Cryst.* A**53**, 28–34.
Stetsko, Yu. P. & Chang, S. L. (1999). *Acta Cryst.* A**55**, 683–694.
Stetsko, Yu. P., Chang, S. L., Juretschke, H. J., Huang, Y. S., Chao, C. H. & Chen, C. K. (1999). *Phys. Rev. Lett.* (LH7150), unpublished.
Stetsko, Yu. P., Juretschke, H. J., Huang, Y. S., Chao, C. H., Chen, C. K. & Chang, S. L. (2000). *Acta Cryst.* A**56**, 394–400.
Thorkildsen, G. (1987). *Acta Cryst.* A**43**, 361–369.
Weckert, E. & Hümmer, K. (1997). *Acta Cryst.* A**53**, 108–143.
Weckert, E., Schwegle, W. & Hümmer, K. (1993). *Proc. R. Soc. London. Ser. A*, **442**, 33–46.
Wagner, E. (1923). *Phys. Z.* **21**, 94–98.